Monte Carlo simulation of liquid bridge rupture: Application to lung physiology

Adriano M. Alencar,[1] Elie Wolfe,[2] and Sergey V. Buldyrev[2]
[1]*Harvard School of Public Health, Harvard University, Boston, Massachusetts, 02115, USA*
[2]*Department of Physics, Yeshiva University, New York, New York, 10033, USA*
(Received 23 March 2005; revised manuscript received 23 June 2006; published 31 August 2006)

In the course of certain lung diseases, the surface properties and the amount of fluids coating the airways changes and liquid bridges may form in the small airways blocking the flow of air, impairing gas exchange. During inhalation, these liquid bridges may rupture due to mechanical instability and emit a discrete sound event called pulmonary crackle, which can be heard using a simple stethoscope. We hypothesize that this sound is a result of the acoustical release of energy that had been stored in the surface of liquid bridges prior to its rupture. We develop a lattice gas model capable of describing these phenomena. As a step toward modeling this process, we address a simpler but related problem, that of a liquid bridge between two planar surfaces. This problem has been analytically solved and we use this solution as a validation of the lattice gas model of the liquid bridge rupture. Specifically, we determine the surface free energy and critical stability conditions in a system containing a liquid bridge of volume Ω formed between two parallel planes, separated by a distance $2h$, with a contact angle Θ using both Monte Carlo simulation of a lattice gas model and variational calculus based on minimization of the surface area with the volume and the contact angle constraints. In order to simulate systems with different contact angles, we vary the parameters between the constitutive elements of the lattice gas. We numerically and analytically determine the phase diagram of the system as a function of the dimensionless parameters $h\Omega^{-1/3}$ and Θ. The regions of this phase diagram correspond to the mechanical stability and thermodynamical stability of the liquid bridge. We also determine the conditions for the symmetrical versus asymmetrical rupture of the bridge. We numerically and analytically compute the release of free energy during rupture. The simulation results are in agreement with the analytical solution. Furthermore, we discuss the results in connection to the rupture of similar bridges that exist in diseased lungs.

DOI: 10.1103/PhysRevE.74.026311 PACS number(s): 47.90+a, 04.60.Nc, 04.20.Fy, 89.20.−a

I. INTRODUCTION

The scientific study of capillary liquid bridges has been a classical problem for more than a century [1], attracting interest in physics and physiology [2–4], with numerous publications on equilibrium and linear stability problems [5,6]. The shape, stability, and rupture conditions of the liquid bridge are strongly influenced by surface tensions at the air-liquid interface and the nature of the solid-liquid contact. Liquid bridges are of interest because of their importance in industrial processes such as zone refining, low gravity technology, and lung mechanics.

In the specific case of the lung airways, which are coated with a mixture of organic fluids, the surface forces play a major role in the breathing mechanics. In the course of certain lung diseases, the surface properties of these fluids are changed and liquid bridges may form in small airways, blocking the flow of air, and impairing gas exchange [7–10]. During inhalation, liquid bridges may rupture due to mechanical instabilities [11,12] and emit a discrete sound event called *pulmonary crackle*, which can be heard using a simple stethoscope. This can assist in pulmonary diagnostics [13–18]. The emission of this sound has been modeled as a stress quadrupole and compared with experimental data recorded at the chest wall [19], and modeled as a pressure spike propagating through the airway tree [17]. However, no quantitative analysis of the rupture of such bridges and the associated sound release has been provided. We hypothesize that this sound is a result of the acoustical release of the energy that had been stored in the surfaces of liquid bridges prior to their rupture, and develop a lattice gas model capable of describing these phenomena. Real airways have complex topology and the coating fluids have complex mechanical properties. Furthermore, there is an air pressure difference on the opposite sides of the bridge. As a step toward modeling this process, we address a simpler but related problem, a liquid bridge between two planar surfaces. This problem can be analytically solved [20–27] and we use this analytical solution as a validation for the model, which is needed, since the simulations deal with a finite number of elements and thus we might expect strong finite size effects on its results.

We study the stability of axially symmetrical liquid bridges between two semiwet planes, where the base radius R at both planes is not fixed. Although similar problems have received much attention, the dependence of the energy gap between closed and open states on contact angle Θ and surface tension, has not been theoretically explored. The equilibrium and stability of such liquid bridges are usually quantified by the slenderness Λ (or aspect ratio),

$$\Lambda = \frac{h}{R}, \tag{1}$$

where $2h$ is the separation between the two planes (see Fig. 1). For this particular geometry, we can distinguish two stable configurations: (i) when the liquid phase forms a bridge between the two planes, *closed state* [Figs. 1(a) and 1(b)], and (ii) when the liquid phase forms droplets on the planes, *open state* [Figs. 1(c) and 1(d)].

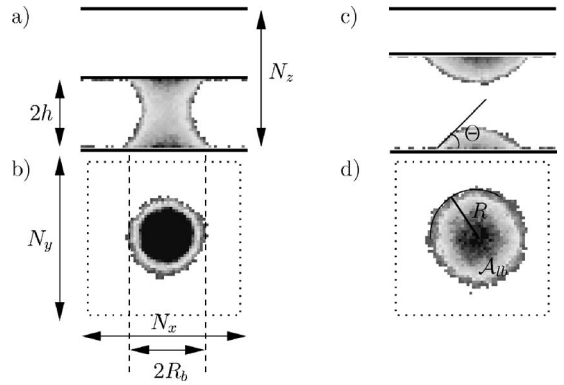

FIG. 1. Illustrative example of the liquid bridge between two parallel planes. N_x, N_y, and N_z are the linear dimensions of the lattice. $2h$ is the separation between the two planes, $\mathcal{A}_{lb}$ and $R=\sqrt{\mathcal{A}_{lb}/\pi}$ are, respectively, the area and the radius of an arbitrary z layer, and R_b is the radius of the base. (a) x-z planar view and (b) x-y planar view of the closed state. (c) and (d) are the same views for the open state. The gray scale indicates the number of molecules in the projection. Both the large number and small number are shown as a darker gray.

We develop a lattice gas model to simulate liquid bridge rupture based on a set of local rules of transitions (Sec. II). In addition to the lattice gas simulation, we solve this problem using numerical integration of variational equations describing the liquid bridge at the equilibrium (Appendix A). For several contact angles Θ, we obtain the energy of the system, geometry of the bridge, the condition of the stability of the bridge, and the critical conditions of the symmetric versus asymmetric rupture of the bridge. The agreement between the lattice gas model and the results obtained by variational calculus is used to validate the model and interpret its results (Sec. III).

II. LATTICE GAS MODEL

Our system is defined by a cubic lattice with all sites occupied with particles of type p, where $p=g$ represents a gas, $p=l$ a liquid, and $p=s$ a solid wall particle. In the Monte Carlo (MC) simulations, a given configuration evolves toward a typical equilibrium configuration by the Metropolis algorithm, in which many small transitions in molecular configuration occur sequentially [28,29]. The transitions are implemented by exchanging the liquid and gas particles of any two sites following the Kawasaki dynamics [30,31]. The walls are modeled with solid particles that are not allowed to move. The probability that a given transition will occur depends on the corresponding energy cost resulting from the transition. For a given temperature T, a transition that reduces the potential energy of the system occurs with probability 1, while a transition that increases the potential energy by $\Delta E>0$ occurs with probability $\Pi=\exp(-\Delta E/k_BT)$, where k_B is the Boltzmann constant.

For a given site m, the energy E_m is

$$E_m = J\sum_{k=0}^{n} s_{ij}, \tag{2}$$

where $i=p(m)$, $j=p(k)$, are the types of particles at sites m and k, $n=26$ is the number of neighbors with 6 particles at a distance of 1, 12 particles at a distance of $\sqrt{2}$, and 8 particles at a distance of $\sqrt{3}$. The value of the pair potential energy s_{ij} is determined from Table I. In order to model the long-range solid-liquid and liquid-liquid interactions, we assume that the particles with distance $\sqrt{3}$ have twice as weak interactions than the rest of the neighbors. In contrast, the interactions with gas particles are restricted to neighbors with distance $\leqslant\sqrt{2}$. In all of our simulations, the number of particles of each type, the temperature, and the volume of the system are constant (canonical ensemble).

TABLE I. The interaction values of the parameter s_{ij} between the three elements of the system, for a contact angle of 45°, where i and j correspond to the two interacting particles.

	Gas	Liquid	Solid
Gas	$s_{gg}=0$	$s_{gl}=-0.02$	$s_{gs}=-0.032$
Liquid	$s_{lg}=s_{gl}$	$s_{ll}=-1.0$	$s_{ls}=-1.45$
Solid	$s_{sg}=s_{gs}$	$s_{sl}=s_{ls}$	

The system lattice has fixed size $N=N_x\times N_y\times N_z$, with three planes of solid particles forming walls at $Z=0$, $Z=2h$, $Z=N_z$, and periodic boundary conditions in X and Y planes. The three planes divide the system into two containers (see Fig. 1); the bottom container with $0<Z<2h$ and the top container with $2h<Z<N_z$. The particles in the top container do not interact with the walls, so no condensation occurs in it. The plane $Z=2h$ can move up and down between different simulations reducing the size of one of the containers and increasing the size of the other, such that the total volume and the number of particles always remain constant.

The simulation starts with a cylindrical liquid bridge with initial radius R consisting of $N_\ell\approx 10^4$ particles of liquid positioned at the center of the xy plane inside the bottom container. From the initial configuration the system is let to relax until it reaches the steady state. Figure 2 shows the relaxation process for the aspect ratio Λ and contact angle Θ as a function of the number of MC steps, where one MC step is equivalent to N_ℓ molecular transitions.

This numerical simulation is repeated for fixed N_ℓ and for different values of h. For $h\leqslant h_c$ the system relaxes into a liquid bridge configuration, while for $h>h_c$ the liquid bridge breaks, forming either one droplet or two droplets on opposite walls. At the critical point $h=h_c$, the contact angle, the shape of the liquid bridge, the surface area, and the potential energy are recorded. The same set of simulations is then repeated for different interaction parameters s_{ls}, which allows us to simulate systems with different contact angles (see Fig. 3).

The parameters of interaction between neighbors are given in Table 1. We compute the effect of the solid-liquid interaction parameter s_{12} on the contact angle by two distinct methods. In the first method, we compute the area $\mathcal{A}_{lb}(\delta z)$ of the three consecutive parallel layers of the liquid bridge characterized by distances $\delta z=1/2$, $3/2$, and $5/2$ to the planes. From the area of each layer, we compute its average radii $R(\delta z)=\sqrt{\mathcal{A}_{lb}(\delta z)/\pi}$ (see Fig. 1). For each simulation we compute two contact angles $\Theta_\pm$ with the top and bottom

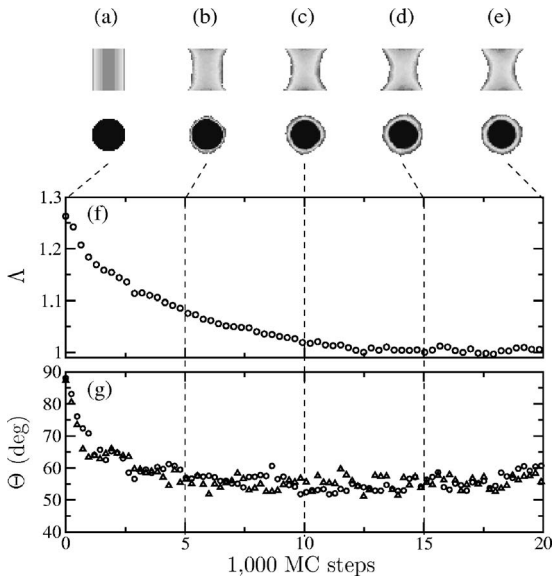

FIG. 2. The projections of the bridge on Y and Z planes during the relaxation process for $\Theta=50°$ from (a), the initial configuration, to (e) after 20,000 MC steps. (f) The aspect ratio Λ and (g) contact angle Θ during the relaxation process, where circles and triangles denote the contact angle at the bottom and the top of the liquid bridge.

parallel planes, fitting by a straight line the three radii $R(\delta z)$ versus δz. Averaging these two values we find Θ (see the filled circles in Fig. 3). In the second method, we build six new systems to estimate the surface tension of the liquid-gas γ_{lg}, of the gas-solid γ_{gs}, and of the liquid-solid γ_{ls}, interfaces, respectively. We build the three pairs of systems such that in each pair the area of the desired interface is changed but the total volume of particles of each type is exactly the same (see Fig. 4). Then, the surface tension is estimated as

$$\gamma = dU/d\mathcal{A}_{slab},$$

where dU is the total change in potential energy and $d\mathcal{A}_{slab}$ is the change in the surface area between the two constitutive

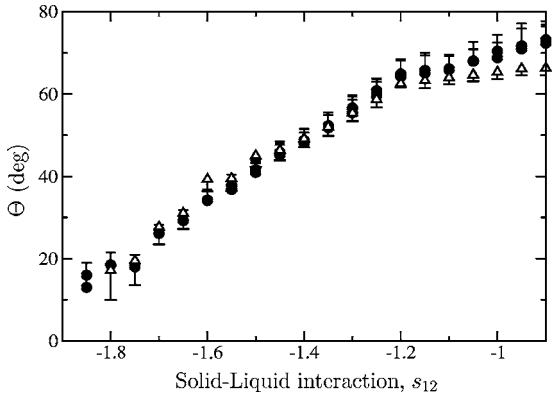

FIG. 3. The interaction values of the parameter s_{ls} between solid-liquid for different contact angles using two distinct methods. Filled circles are the results measured during the simulations of the liquid bridge, and the open triangles are the results calculated from the definition of surface tension from the six systems illustrated in Fig. 4 using two sizes of boxes $40\times40\times100$ and $20\times20\times400$.

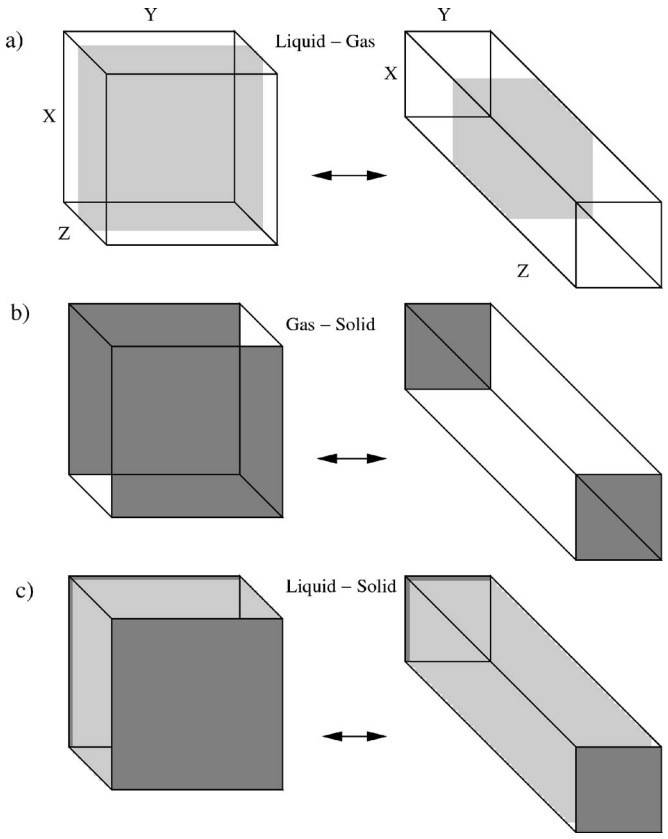

FIG. 4. Schematic drawing of the three pairs of systems used to compute the surface tension of (a) liquid-gas, (b) gas-solid, and (c) liquid-solid. The light gray in (a) represents liquid particles, the dark gray planes in (b) and (c) represent solid walls, and all remaining spaces in (a) and (b) are filled with air. All boxes have the same volume and the members of each pair have exactly the same content.

elements of the system. The contact angle Θ is then found using the Young relation $\cos\Theta=(\gamma_{gs}-\gamma_{ls})/\gamma_{gl}$. The results from both methods are shown in Fig. 3.

Except for the surface tension estimation (see the open triangles in Fig. 3), all the results are presented for the system size $N_x=60$, $N_y=60$, and $N_z=52$, with three planes of solid, and $N_xN_y(N_z-3)=172{,}800$ sites occupied either by a liquid or a gas particle. The temperature used is $k_BT=0.9J$, which allows the MC dynamics to have a reasonable computing time still keeping the liquid with sufficiently large gas-liquid surface tension. For $k_BT\ll0.9J$, the dynamics becomes extremely slow, and for $k_BT\gg0.9J$, the liquid-gas interface becomes rough as the system approaches the liquid-gas critical point. The number of molecules of liquid is $N_\ell=10{,}925$ and $172{,}800-N_\ell$ is the number of gas molecules, thus, only 7% of the containers are occupied by liquid. Note that this percentage does not change when the height $2h$ of the moving plane changes.

We estimate the free energy of the system by computing the total potential energy of all interacting particles, neglecting the entropic term. We also find the liquid-gas surface area for different wall separation while monitoring the shape of the bridge, taking snapshots of the system at each 8000 MC steps (see Fig. 5). We also monitor the shape of

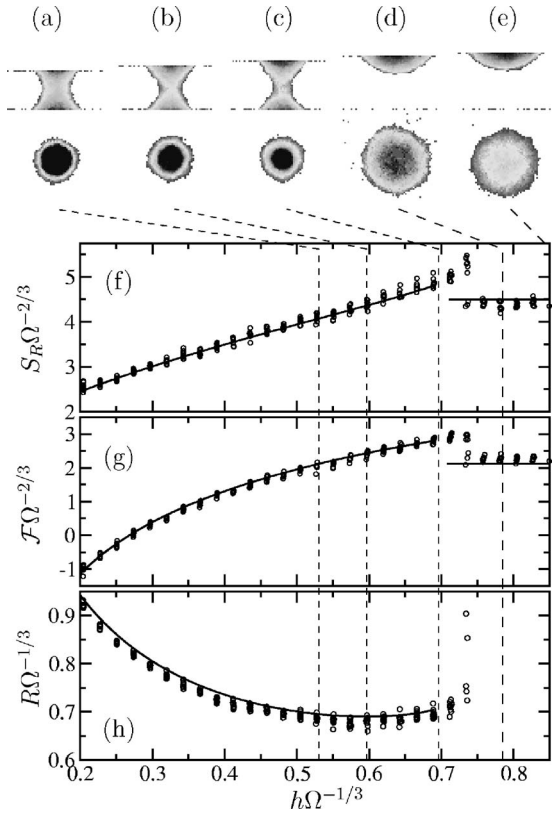

FIG. 5. Screen shots of the simulations of the liquid bridge during the expansion and consequent rupture. (a)–(e) Images and (f)–(h) results from the model simulation (circles and triangles) and from the variational calculus (solid lines). (f) The normalized rotational surface area S_R in comparison with the predictions of Eq. (A25) for the bridge before rupture and Eq. (A56) for the droplet after rupture for $\Theta=50°$, as a function of the normalized half-distance h; (g) the respective results for the normalized total free energy $\mathcal{F}$, in comparison with Eq. (A28) for the bridge before the rupture and Eq. (A57) for the droplet after the rupture; and (h) the respective result for the normalized radius of the bases of the liquid bridge [Eq. (A23)]. Filled triangles are the normalized R at the top of the bridge and open circles are the normalized R at the bottom. For the analytic results, the parameter a is found as the largest root of Eq. (A22) for a given normalized half-distance $\eta=h\Omega^{-1/3}$. The graphs for the analytical solutions are terminated as η reaches $\eta_{ms}=0.69$ [the limit of the bridge mechanical stability determined from Eq. (A51)], since $\Theta=50°$ is larger than $\Theta_c\approx 31°$. The variational stability analysis also predicts that for $\Theta>\Theta_c$, the bridge must rupture asymmetrically forming a single droplet, which is indeed observed in the simulations (see Fig. 8).

the bridge for different values of Θ at the maximal h, for which the bridge remains stable by measuring the average radius $\rho(z)$ of the bridge as a function of coordinate z (see Fig. 7).

Although we simulate the system at a constant number of liquid particles, the number of particles forming either the bridge or the droplet depends on the surface geometry, since the equilibrium vapor pressure P_H [32] depends on the average curvature of the interface H,

$$P_H \propto \exp(cH), \tag{3}$$

where $c=2\gamma_{lg}/kTn_0$ is a parameter that depends on the liquid-gas surface tension γ_{lg}, temperature T, and the number density of the liquid bridge n_0. The curvature of the liquid bridge is smaller than the curvature of the droplets, thus the equilibrium vapor pressure near the bridge is smaller than near the droplet, and since the total number of the liquid particles is constant, some particles forming the bridge must evaporate when the bridge breaks into droplets. In most physical cases, the evaporation is much slower than the mechanical changes in the system, such as the increase of the separation between the planes, thus this situation roughly corresponds to a fixed volume of the liquid phase during the breaking. In our simulation, we do observe small changes in the volume of the liquid phase, but these changes will be neglected in the analytical calculations.

III. RESULTS

We use a lattice gas model and analytical calculation (see Appendix A) to study critical conditions of the liquid bridges rupture. We express all relevant characteristics of the bridge in terms of elliptic integrals which depend on the contact angle Θ and the bridge neck to base ratio $a=A/R$, where A is the radius of the neck of the bridge. For each dimensionless plane separation $\eta=h\Omega^{-1/3}$ and Θ, we can uniquely determine parameter a as the largest root of a transcendental equation (A22). Thus all the characteristics of the bridge can be analytically expressed in terms of η and Θ. Moreover, for each Θ we can find the largest $\eta=\eta_{ms}$, for which the bridge is mechanically stable. It must be taken into account, that for the small systems, which we simulate, the transition from closed to open states happens with probability $p\sim\exp(\delta\mathcal{F}/kT)$, where $\delta\mathcal{F}$ is the free-energy barrier. Thus the transition will not necessarily happen exactly as predicted for an infinitely large system. Thus we observe that sometimes the bridge can break for $\eta<\eta_{ms}$. Also, since we allow the system to equilibrate at each plane separation for only a finite time, the bridge may temporarily survive at $\eta>\eta_{ms}$ even though it would break at these separations if we equilibrated the system for a sufficiently long time. Nevertheless, we find remarkable agreement between the simulation and the analytical results.

During the stretching of the liquid bridge by pulling the upper plane (see Fig. 5), the liquid-air surface of the liquid bridge changes according to Fig. 5(f), the base radius changes according to Fig. 5(h), and the free energy monotonically increases [see Fig. 5(g)]. We also find that for $\Theta<65°$, the radius of the bases of the liquid bridge behaves nonmonotonically with the increase of plane separation reaching a minimum, after which the radius of the bases starts to increase until the liquid bridge breaks [see Fig. 5(h)]. This counterintuitive observation is in complete agreement with the analytical calculations. Indeed, using Eq. (A23) to compute R, we find that R reaches its minimum as a function of η at $\eta<\eta_{ms}$ if $\Theta<65°$.

The increase in energy comes from the force that is required to pull the plane and is stored at the surface of the

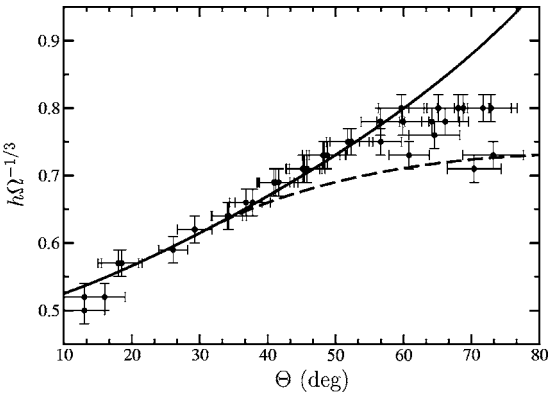

FIG. 6. Maximal half-distance between the two plates, at which the bridge is mechanically stable, computed using Eq. (A52) (solid line) for $\Theta<\Theta_c$ and Eq. (A51) for $\Theta<\Theta_c$ (dashed line). Circles indicate the value of h for which the bridge breaks during the first 400,000 MC steps of the simulation. During each MC step, the algorithm randomly visits N_ℓ particles. The horizontal error bar is obtained by measuring the values of the contact angle for eight configurations taking each 4,000 MC steps after the system reaches the equilibrium. The vertical error bars correspond to 1 lattice cell resolution for the distance at which the rupture is observed.

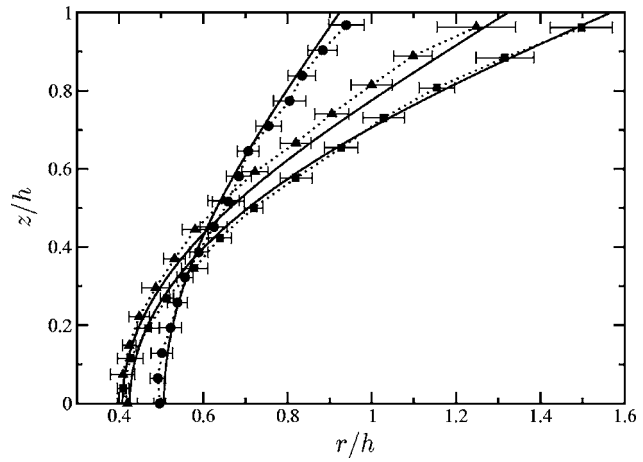

FIG. 7. The minimal stable rotational surface at various Θ from the model $\Theta=25°$ (filled square), 34° (filled triangles), and 57° (filled circles), and the respective values from the variational calculation, using Eqs. (A13) and (A26) in which $a=a_0$ for $\Theta<\Theta_c$ and $a=a_c=\tan(\Theta/2)$ for $\Theta>\Theta_c$.

liquid bridge as a consequence of the increase on its surface area. Since the free energy of one or two droplets formed from the liquid bridge after its rupture is smaller than the free energy of the stretched liquid bridge, the excess energy $\Delta\mathcal{F}$ stored in the surface of the bridge is abruptly released to the system. We hypothesize that most of this energy is released in the form of mechanical perturbation, i.e., acoustic waves. In Ref. [19], it was suggested that the acoustic energy results from the relaxation of the stress accumulated in the tissues around the closed airways in comparison to the opened airways. However, an elementary analysis of the system consisting of two elastic springs with different spring constants connected in series shows that the potential energy stored in each of the springs is inversely proportional to its spring constant. Clearly, an airway blocked by a liquid bridge can be represented by such a system, in which the spring with the smaller spring constant represents the liquid bridge and the spring with the larger spring constant represents tissue. Thus, the major part of the potential energy of such a system is stored in the bridge and not in the tissue. Accordingly, we suggest the energy of the acoustic wave can be estimated as $\Delta\mathcal{F}$. For the liquid bridge between two parallel planes, the quantity $\Delta\mathcal{F}$ can be found analytically and is given in Sec. 7 of the Appendix.

The contact angle Θ is the main parameter, which determines the critical separation between the planes $2h_c$ where the liquid bridge breaks (see Fig. 6). It also determines the shape of the liquid bridge (see Fig. 7) at the point of rupture. We found the maximal plane separation, where the bridge is mechanically stable as a function of Θ, determined from two different conditions, namely, Eqs. (A52) for $\Theta<\Theta_c$ and (A51) for $\Theta>\Theta_c$. For $\Theta>\Theta_c$, the liquid bridge breaks via an asymmetrical fluctuation that shifts the neck of the bridge towards one of the planes, which results in the formation of a single droplet attached to one of the planes. This takes place when the bridge profile develops inflection points near the planes [20]. For $\Theta<\Theta_c$, the bridge breaks symmetrically by narrowing its neck [20] and forming two equal droplets at the opposite planes. To quantitatively characterize the asymmetry of the breaking process in simulations, we introduce an asymmetry parameter $(h_1+h_2)/h_1$, where $h_1>h_2$ are the distances from the neck of the bridge to the opposite planes $(h_1+h_2=2h)$ just before the rupture (Fig. 8). We found that for $\Theta<30°$, the asymmetry parameter is close to 2.0, while for $\Theta>30°$, it starts to decrease and approaches 1.0 for $\Theta\to 90°$ in agreement with the analytical predictions.

At the line of mechanical instability, the free energy of the bridge is larger than the free energy of the droplets (see Fig. 9) so the bridge can still break if it develops a large enough

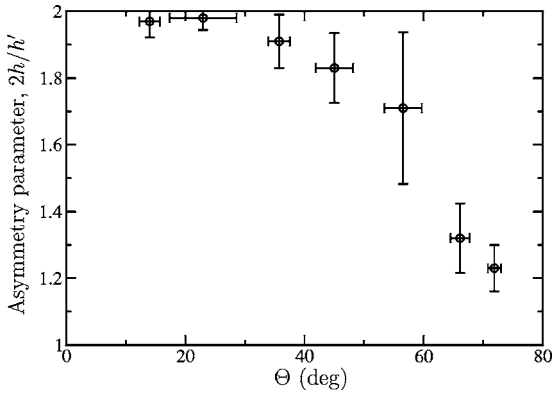

FIG. 8. Asymmetry parameter of the liquid bridge defined as $2h/h_1$, where h_1 is the largest among two distances between the neck of the bridge and the two plates just before the rupture. Values of this parameter near two indicate the liquid bridge will break symmetrically, forming two droplets. All values significantly below two indicates the bridge will break asymmetrically and form a single droplet or two droplets with one of them being very small compared to the other.

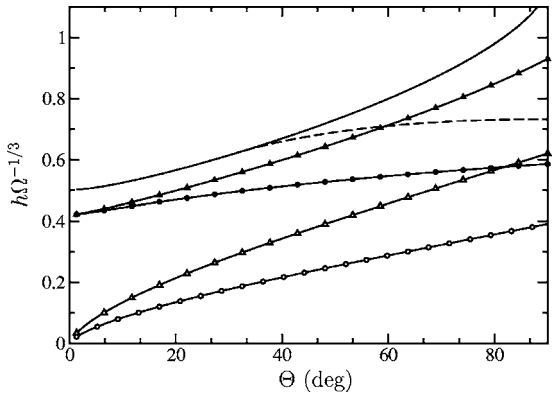

FIG. 9. Dependence on the contact angle Θ of the maximal separation between planes $h_{\max}=h(a_0)$ (solid line) for which the solutions of Eq. (A22) exist. $h_c(\Theta)$ (dashed line) is the maximum separation for which the bridge is mechanically stable. $h_{\min,1}$ (open circles) and $h_{\min,2}$ (open triangles) are the minimal separation for one and two droplets, respectively. $h_{s,1}$ (filled circles) and $h_{s,2}$ (filled triangles) are the values of h, for which the free energy of the bridge is equal to the free energy of one and two droplets, respectively.

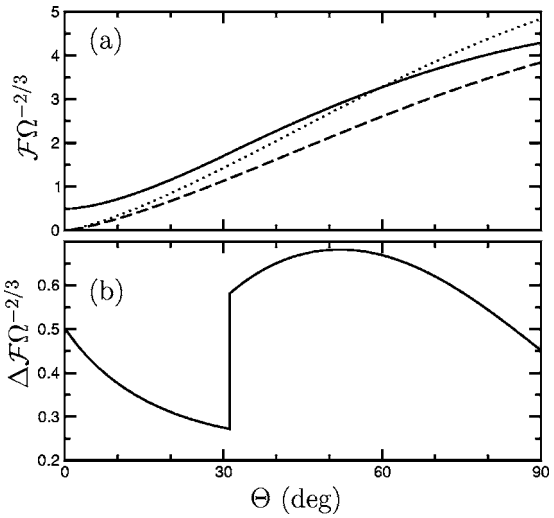

FIG. 10. (a) The maximal free energy of the bridge $\mathcal{F}[h_c(\Theta)]$, as a function of the contact angle Θ. Also shown are the free energies $\mathcal{F}_{0,1}$ of one droplet (dashed line) and $\mathcal{F}_{0,2}$ of two droplets (dotted line). (b) The free energy difference $\Delta\mathcal{F}=\mathcal{F}-\mathcal{F}_{0,k}$ between the closed and the opened states, where $k=2$ for $\Theta<\Theta_c$ and $k=1$ for $\Theta>\Theta_c$.

fluctuation, which allows it to overcome the free energy barrier. In the microscopic system which we simulate it may happen spontaneously. Above the mechanical stability line the bridge inevitably breaks, but the characteristic breaking time, which depends on the viscosity of the fluid and the bridge volume, may be larger than the time we allow the bridge to equilibrate at each plane separation. Note the bifurcation of the simulation results for the base radius close to the breaking point when the plane separation exceeds the theoretical limit of stability. This bifurcation indicates that the bridge has already become asymmetric, which must take place before the asymmetric rapture predicted for $\Theta>31°$.

In certain lung diseases, such as pneumonia, the liquid layer that coats the internal surface of the airways has its surface properties changed leading to the formation of liquid bridges inside the small airways, which block the flow of fresh air to the alveoli, where the gas exchange occurs. During a deep breath, an overexpansion of the lung may open these blocked airways by breaking the liquid bridges inside them and an acoustic noise (called pulmonary crackles) can be heard with the help of a stethoscope. The frequency and intensity of these acoustic waves are associated with different diseases or different stages of a given disease. In this context, our observation that the free energy $\Delta\mathcal{F}$ release and the dynamics of rupture abruptly changes at $\Theta\approx31°$ (Fig. 10), may correspond to the change in the pulmonary crackles strength and shape as the properties of coating fluids change as the disease progresses. However, our model in its present state cannot be directly applied to the lung physiology, mainly due to the topological difference between the bridge we study and the bridge in the airways that is formed by two spherical menisci. Also, the liquid bridge in the airways breaks not only due to geometrical expansion, but also due to the pressure difference across its sides. In addition, a complex mixture of organic fluids coating the airways may not be treated as a Newtonian fluid. Thus, a direct comparison between the energy released during the rupture of liquid bridges in lung airways and the system that we use here is not straightforward. However, the numerical algorithm which is a standard lattice gas model with low computational cost can easily be implemented in arbitrary geometries and mixtures of particles. The main conclusion of our work is that the lattice gas method gives accurate results in a situation that can be tested analytically and thus, can be reliably used in more complex situations, such as where the analytical solutions do not exist. The connection between the surface properties of the fluids in the lung and the acoustic noise generated during the liquid bridge rupture is crucial for understanding the pathology of several diseases and for improving clinical diagnoses. In conclusion, we quantitatively analyze a physical mechanism for the energy accumulation and release necessary for the formation of acoustic waves and find a pathway to simulate more complex systems than those used in this paper.

ACKNOWLEDGMENTS

We thank T. I. Vogel for consulting us on the mathematical aspects of the liquid bridge problem. E. W. and S. V. B. are grateful to Dr. Morton Lowengrub, Vice President for Academic Affairs of Yeshiva University, for his support of undergraduate summer research.

APPENDIX A: VARIATIONAL METHOD

1. Mathematics of the liquid bridge problem

The problem of the equilibrium shapes of capillary surfaces has received much attention in the past few centuries [21,20]. At a constant temperature, the condition for mechanical stability of the system corresponds to the local mini-

mum of the free energy, which means that the free energy of the system can only increase if the surface of the liquid is perturbed by an infinitesimally small perturbation. The problem of the stability of the liquid bridge of a given volume Ω, trapped between two parallel planes with given separation $2h$ and given surface tensions between liquid, gas, and two different solids (in the absence of gravity), has been studied [22–26] and summarized [20].

It is established [20,23,24] that the solution of this problem is an axially symmetric surface that makes certain contact angles Θ_1 and Θ_2 with the planes and is produced by the rotation of a curve $\rho(z)$ $(-h \leqslant z \leqslant h)$ around the z axis, perpendicular to the planes. Such a surface must have constant average curvature $H(\Omega, h, \Theta 1, \Theta 2)$. Rotationally symmetric surfaces with constant average curvature are called Delaunay surfaces. In 1841, Delaunay proved that the curve $\rho(z)$ for a such a surface could be obtained as a trajectory of a focus of an arbitrary conic section rolling along the z axis. If the rolling curve is an ellipse, then $H>0$ and the surface is called unduloid. If the rolling curve is a hyperbola, then $H<0$ and the surface is called nodoid. In the case of a parabola, $H=0$ and the surface is called catenoid, because in this case, $\rho(z)$ has the shape of a chain line.

In the case of equal contact angles (planes are made of the same material), the necessary and sufficient conditions for the stability of a liquid bridge of volume $\Omega=\Omega_0$ between two parallel planes separated by a fixed distance $2h$ are (i) the surface of the bridge must be a rotationally symmetric Delaunay surface of constant average curvature H, (ii) its profile must have no inflections $[\rho''(z) \neq 0]$ in the interval $[-h, h]$, and (iii) its profile must belong to a continuous family of solutions for which $\partial\Omega/\partial H<0$ for any $\Omega \geqslant \Omega_0$. These conditions follow from the theorems proved by Vogel and Finn [22–24], see also Ref. [20]. From conditions (i) and (ii) it follows that the stable bridge must be symmetric with respect to $z=0$: $\rho(z)=\rho(-z)$. Langbein [20] have shown that for $\Theta<\Theta_c \approx 31.15°$, the bridge of fixed volume Ω loses its stability (as the separation between the planes increases) exactly at the point when $\partial\Omega/\partial H=0$ due to a symmetric variation, while for $\Theta>\Theta_c$ the bridge loses stability when the inflection points appear at the boundary $\rho''(-h)=\rho''(h)=0$ due to an antisymmetric variation. Exactly at $\Theta=\Theta_c$, both conditions are satisfied and the bridge can break either symmetrically or antisymmetrically. Also, Finn and Vogel [24] have proved the Carter conjecture [27], namely, that $\Omega=8h^3/\pi$ is the volume infimum for the set of all stable bridges, which is reached at $\Theta=\pi/2$.

Here we will deal with the situation $\Theta_1=\Theta_2=\Theta \leqslant \pi/2$ in detail. We will derive the explicit expressions for the bridge profile and for the free energy in terms of elliptic functions. We will explicitly find the limits of the bridge stability as functions of Θ, and determine the shape of the bridge instability that causes the rupture of the bridge both above and below Θ_c. We will show that for $\Theta>\Theta_c$, the bridge breaks antisymmetrically, forming a drop attached to one of the planes, while for $\Theta>\Theta_c$, it breaks symmetrically into two equal drops on the opposite planes. We also present a new derivation of the expression of which $\Theta=\Theta_c$ is the root and determine a complete phase diagram of the bridge stability on the (Θ, η) plane where $\eta=h\Omega^{-1/3}$ is the dimensionless plane separation related to the dimensionless volume $\omega \equiv (\Omega/2\pi h)=(2\pi\eta^3)^{-1}$.

2. Free energy functional

Following Refs. [20,22–24], we seek the equilibrium shape of the bridge as the rotational surface, produced by the rotation of the curve $\rho(z)$ around the z axis perpendicular to the planes. The surface free energy of the problem is then given by

$$\gamma_{gl}S_R + \gamma_{ls}S_B + \gamma_{sg}(S_T - S_B) + c, \tag{A1}$$

where S_R is the rotational surface of the bridge, $S_B=\pi[\rho^2(-h)+\rho^2(h)]$ is the area of the liquid-solid interface, S_T is the total surface of the planes (which is constant), and c is an arbitrary additive constant. In the following, we will denote for brevity, the liquid gas surface tension $\gamma \equiv \gamma_{gl}$. Taking into account the conditions of mechanical stability $\gamma_{sg}-\gamma_{sl}=\gamma\cos\Theta$, and selecting $c=-S_T\gamma_{sg}$, we obtain the expression for the total free energy

$$\mathcal{F} = \gamma[S_R + \cos\Theta S_B] = \gamma\pi\left\{2\int_{-h}^{h}\rho\sqrt{1+\rho'^2}dz + \cos\Theta[\rho^2(-h)+\rho^2(h)]\right\}. \tag{A2}$$

In order to find the equation of the surface with given volume Ω, we will minimize the functional [33]

$$\mathcal{F} - 2\gamma H\Omega = \gamma\pi\left\{2\int_{-h}^{h}(\rho\sqrt{1+\rho'^2} - H\rho^2)dz + [\rho^2(-h) + \rho^2(h)]\cos\Theta\right\}, \tag{A3}$$

where the first term of the integral part is the rotational surface and the second term is the volume

$$\Omega = \pi\int_{-h}^{h}\rho^2(z)dz \tag{A4}$$

multiplied by a Lagrange multiplier, $\lambda=2\gamma H$. The contribution of the solid-liquid contact area is automatically taken into account if we impose transversal conditions on the derivatives of the profile at the contact points

$$\rho'(-h) = \rho'(h) = \pm\cot\Theta. \tag{A5}$$

The Lagrangian of this problem is

$$\mathcal{L} \equiv 2\pi\gamma(\rho\sqrt{1+\rho'^2} - H\rho^2).$$

Since the Lagrangian does not depend on z, the Hamiltonian

$$\mathcal{H} = \mathcal{L} - \mathcal{L}_{\rho'}\rho'$$

is the integral of the correspondent Euler's differential equation,

$$\mathcal{E}(\rho) \equiv -\frac{\rho''}{(\sqrt{1+\rho'^2})^3} + \frac{1}{\rho\sqrt{1+\rho'^2}} = 2H. \tag{A6}$$

Thus, we have

$$\mathcal{H} = 2\pi\gamma\frac{\rho}{\sqrt{1+\rho'^2}} - 2\gamma H\pi\rho^2 = T, \tag{A7}$$

where an arbitrary constant T is the force needed to hold the two planes apart, and H has the meaning of the average curvature. Indeed, the first term of the left-hand side of Eq. (A7) has the physical meaning of the projection of the force created by surface tension on the z axis, while the second term has the meaning of the force created by Pascal pressure $2\gamma H$ inside the interface with average curvature H. The right-hand side has the physical meaning of the total force acting on a horizontal section of the bridge, which must be constant along the z axis to keep the mechanical stability. One can show that $T>0$ for any bridge for which $\rho(z)$ achieves minimum at $z_0 \in (-h,h)$. Indeed, let us denote $\rho_1 \equiv 1/\rho''(z_0)$, the radius of curvature of the profile of the bridge at z_0, and $\rho_0=\rho(z_0)$, the radius of the neck of the bridge. Then, $H=(1/\rho_0-1/\rho_1)/2$ and $T=2\pi\gamma(\rho_0-\rho_0^2H) = \pi\gamma(\rho_0+\rho_0^2/\rho_1)>0$. Even if the bridge has a maximum in $(-h,h)$, we still have $T>0$ for $-\rho_1>\rho_0$. If the surface of the bridge is spherical ($\rho_1=-\rho_0$), we have $T=0$, i.e., there are no external forces which distort the minimal surface of the droplet. Thus, $T<0$ only if $-\rho_1<\rho_0$, i.e., the droplet is squeezed between the plates, which can be the case for $\Theta>\pi/2$.

3. Solving the Euler's equation

Equation (A7) can be rewritten in the form

$$\frac{\rho}{\sqrt{1+\rho'^2}} = H\rho^2 + C, \tag{A8}$$

where H and $C=T/(2\pi\gamma)>0$ are two arbitrary constants. Solving Eq. (A8) with respect to dz we have

$$d\rho\frac{H\rho^2+C}{\sqrt{\rho^2-(H\rho^2+C)^2}} = \pm dz.$$

To simplify the problem, we can introduce two new constants $0<A<|B|$, which are the roots of the denominator, such that

$$AB = C/H \tag{A9}$$

and

$$A^2 + B^2 = 1/H^2 - 2C/H. \tag{A10}$$

The roots A and $|B|$ play the role of the minimal and maximal possible distances from the surface of the bridge to the z axis. Note that the sign of B is determined by the sign of the average curvature: $s \equiv \mathrm{sign}(B)=\mathrm{sign}(H)$, i.e, B is positive for the unduloids, B is negative for nodoids, and $B=\infty$ for a catenoid.

Integrating from the position of the "neck" of the bridge z_0, such that $\rho(z_0)=A$, we have

$$z(\rho) = \pm s\int_A^\rho \frac{dx(AB+x^2)}{\sqrt{(B^2-x^2)(x^2-A^2)}} + z_0, \tag{A11}$$

where $+$ corresponds to $z>z_0$ and $-$ corresponds to $z<z_0$. This equation provides the general solution of the Euler's equation (A6). Now our goal is to find constants A, B, and z_0 to satisfy conditions (A4) and (A5).

Differentiating Eq. (A11) with respect to ρ and using $z'=\pm\tan\theta(\rho)$, we find

$$\sin\theta(\rho) = \pm\frac{AB+\rho^2}{\rho(A+B)}, \tag{A12}$$

from which it follows that for a nodoid ($B<0$), the angle θ between the surface of the bridge and the plane $z=\mathrm{const}>z_0$ can only decrease from $\pi/2$ at the neck of the bridge $\rho=A$, to 0 at $\rho=\sqrt{-AB}$. Thus the only possible solution for $B<0$ is the symmetric one: $z_0=0$ and $\rho(h)=\rho(-h)$. For the unduloid $B>0$, θ can oscillate an infinite number of times between $\pi/2$ at $\rho=A$ and $\rho=B$ and its minimum $\theta=\arcsin[2\sqrt{AB}/(A+B)]$ at $\rho=\sqrt{AB}$, which corresponds to an inflection point of the profile $z''(\rho)=0$.

4. Symmetric solution

Although asymmetric solutions $z_0\neq 0$ as well as solutions with several waves in the profile $\rho(z)$ are possible, they are all unstable according to the Vogel's theorem since they all have inflection points. So, first we will find the symmetric solution $z_0=0$. Next, we will also find the asymmetric solution since it has a special meaning in the stability analysis of the bridge and also illustrates how our method of finding integration constants can be used in the general case.

In order to satisfy boundary conditions (A5), we must find constants A and B and some unknown radius R, such that $z(R)=\pm h$, $z'(R)=\pm\tan\Theta$. The third equation to define three unknowns A, B, and R, is the condition of a given volume (A4). Introducing the dimensionless variables $a\equiv A/R$, $b\equiv B/R$, $r\equiv\rho/R\in[a,1]$, and

$$u(a,r) \equiv s\frac{z(\rho)}{R} \equiv s\int_a^r \frac{(ab+x^2)dx}{\sqrt{(x^2-a^2)(b^2-x^2)}}, \tag{A13}$$

and using notation

$$\Lambda(a) \equiv u(a,1) = h/R, \tag{A14}$$

we have

$$z(\rho) \equiv \pm\frac{hu(a,\rho\Lambda/h)}{\Lambda},$$

so that $z[h/\Lambda]=\pm h$. The equation for contact angle,

$$\left.\frac{dz}{d\rho}\right|_{\pm h/\Lambda} = \pm\tan\Theta, \tag{A15}$$

allows us to express b and s in terms of the single dimensionless unknown a ($0\leqslant a\leqslant 1$),

$$b(a) = \left(\frac{1-a\sin\Theta}{\sin\Theta-a}\right), \tag{A16}$$

$$s = \begin{cases} 1, & a < \sin\Theta \\ -1, & a > \sin\Theta. \end{cases} \tag{A17}$$

In general, the integral, Eq. (A13), is an elliptical function. In a special case $a \to \sin\Theta$, $b \to \infty$, the integral can be expressed in logarithms, and the surface becomes a catenoid [25].

Using Eqs. (A9) and (A10), we have

$$H = \frac{(\sin\Theta - a)\Lambda}{h(1-a^2)}. \tag{A18}$$

The force $T = 2\pi\gamma C$ is expressed in terms of a as follows:

$$T = 2\pi\gamma a \frac{h(1 - a\sin\Theta)}{(1-a^2)\Lambda}. \tag{A19}$$

From partial integration $\pi u^2(a,r) - 2\pi\int_0^r u(a,x)x dx = \pi\int_0^r x^2 du$, it follows that the volume formed by the surface $z(\rho)$ and the planes $z = \pm h$ is equal to $2\pi h^3\omega(a)$, where

$$\omega(a) \equiv \frac{v(a,1)}{\Lambda^3}, \tag{A20}$$

and

$$v(a,r) \equiv s\int_a^r \frac{x^2(ab + x^2)dx}{\sqrt{(x^2-a^2)(b^2-x^2)}}. \tag{A21}$$

Thus, a can be found from the equation

$$2\pi h^3\omega(a) = \Omega. \tag{A22}$$

Since $\Lambda(a)$, $b(a)$, and $v(a,1)$ are known functions of a given by Eqs. (A14), (A16), and (A21), respectively, Eq. (A22) contains only one unknown variable a, and can be solved numerically for given h, Ω, and Θ, which solves the problem of finding constants, completely.

Accordingly, we can find the radius of the bases

$$R(a) = h/\Lambda(a) = \left[\frac{\Omega}{2\pi\omega(a)}\right]^{1/3}. \tag{A23}$$

For the studies of the free energy, we also need to find the area of the rotational surface $S_R = 2\pi\sigma(a,1)h^2/\Lambda^2$, where

$$\sigma(a,r) \equiv s\int_a^r \frac{(b+a)x^2 dx}{\sqrt{(x^2-a^2)(b^2-x^2)}} \tag{A24}$$

can be found using elementary formulas for the rotational surface area. One can express $u(a,r)$, $\sigma(a,r)$, and $v(a,r)$ in terms of the Legendre elliptic integrals of the first kind,

$$F(k,\phi) \equiv \int_0^\phi \frac{d\psi}{\sqrt{1 - k^2\sin^2\psi}},$$

and the second kind,

$$E(k,\phi) \equiv \int_0^\phi d\psi\sqrt{1 - k^2\sin^2\psi}.$$

After an elementary variable substitution $\phi_r = \arcsin\sqrt{(b^2-r^2)/(b^2-a^2)}$, we have

$$\sigma(a,r) = (b+a)b\tilde{E}(k,\phi_r) \tag{A25}$$

and

$$u(a,r) = a\tilde{F}(k,\phi_r) + b\tilde{E}(k,\phi_r), \tag{A26}$$

where $k = s\sqrt{b^2-a^2}/b$, $\tilde{F}(k,\phi) = F(k,\pi/2) - F(k,\phi)$, and $\tilde{E}(k,\phi) = E(k,\pi/2) - E(k,\phi)$. Finally, partial integration yields

$$v(a,r) = \{-\mathcal{R}(a,r) - a^2 b\tilde{F}(k,\phi_r) + b[3ab + 2(a^2+b^2)]\tilde{E}(k,\phi_r)\}/3, \tag{A27}$$

where $\mathcal{R}(a,r) = r\sqrt{(r^2-a^2)(b^2-r^2)}$, in particular, $\mathcal{R}(a,1) = \cos\Theta(1-a^2)/(\sin\Theta - a)$, and $\mathcal{R}(a,ab) = a^2b^2\cos\Theta(1-a^2)/(\sin\Theta - a)$. The total surface free energy given by Eq. (A2) is

$$\mathcal{F}(a) \equiv 2\gamma\pi h^2 \frac{2\sigma(a,1) - \cos\Theta}{\Lambda^2}. \tag{A28}$$

It follows from the above that solving Eq. (A22) with respect to a gives us all the properties of the liquid bridge. Thus, we need to investigate the existence and uniqueness of its solutions. We have shown numerically that for any contact angle, $\omega(a)$ is a nonmonotonic function of a with a single minimum at $a = a_0(\Theta)$, which can be found as a single root of the equation

$$\frac{d\omega}{da} = \frac{(A_0\tilde{F}^2 + 2B_0\tilde{F}\tilde{E} + C_0\tilde{E}^2 + 2D_0\tilde{F} + 2E_0\tilde{E} + F_0)(1-a^2)}{\Lambda^4(a^2 - 2a\sin\Theta + 1)(a - \sin\Theta)} = 0, \tag{A29}$$

where A_0, B_0, C_0, D_0, E_0, and F_0 are rational functions of a, $\sin\Theta$, and $\cos\Theta$ given by

$$A_0 = \frac{\sin\Theta a^2[a - \cot(\Theta/2)][a - \tan(\Theta/2)]}{(a - \sin\Theta)},$$

$$B_0 = -\frac{\sin\Theta[1 - 2a\sin\Theta + 2a^2\sin^2\Theta - 2a^3\sin\Theta + a^4][a - \cot(\Theta/2)][a - \tan(\Theta/2)]}{(a - \sin\Theta)^3},$$

$$C_0 = 3\frac{\sin\Theta(1 - a\sin\Theta)^2[a - \cot(\Theta/2)][a - \tan(\Theta/2)]}{(a - \sin\Theta)^3},$$

$$D_0=\frac{\cos\Theta(\sin\Theta-2a(1+\sin^2\Theta)+2a^2(\sin\Theta+\sin^3\Theta)+2a^3\cos^2\Theta-a^4\sin\Theta)}{2(a-\sin\Theta)(1-a\sin\Theta)},$$

$$E_0=-\frac{\cos\Theta(1-a\sin\Theta)(2-\sin^2\Theta+a\sin\Theta-2a^2)}{(a-\sin\Theta)^2},$$

$$F_0=2\cos^2\Theta. \tag{A30}$$

These equations can be obtained by direct differentiation of $\omega(a)=v(a,1)/u(a,1)^3$ using formulas for the derivatives of elliptic functions with respect to k and ϕ [34] and taking into account $db/da=[\cos\Theta/(a-\sin\Theta)]^2$, which follows from Eq. (A16). Thus, for

$$h>h_0\equiv\left[\frac{\Omega}{2\pi\omega(a_0)}\right]^{1/3}, \tag{A31}$$

Eq. (A29) does not have solutions, while for $h<h_0$ we have two solutions $a_1<a_0<a_2$, corresponding to the bridges with the narrow and wide necks, respectively. Due to the relation among free energy and force, $\partial\mathcal{F}/\partial h=T$, and since $T>0$, $\mathcal{F}(h)$ is a monotonically increasing function of h. We can determine $h(a)$ for fixed Ω from Eq. (A22). As we can see, $h(a)$ is a monotonically decreasing function of a for $a>a_0$ and a monotonically increasing function of a for $a<a_0$. Thus, $\mathcal{F}(a)$ reaches its single maximum at $a=a_0$ and

$$\left.\frac{\partial\mathcal{F}}{\partial a}\right|_{a=a_0}=0. \tag{A32}$$

Hence a_0 can also be found from Eq. (A32), which appears to be completely equivalent to Eq. (A29).

5. Asymmetric solution

In the following, we will investigate the stability of these solutions. First, we will show that the solution $a_2>a_0$ bifurcates at $a_2=a_c=\tan(\Theta/2)$ into two asymmetric solutions with $z_0\neq 0$. The asymmetric solutions can be found analogously by introducing the two radii R_+ and R_- such that $z(R_\pm)=\pm h$ and the two dimensionless variables $a=A/R_+$, $b=B/R_+$. Equation (A12) shows that $R_-=AB/R_+$, and thus it corresponds to the dimensionless variable ab. Note that b still satisfies Eq. (A16). Thus, the parameter a can be found from the system of two equations, which give the plane separation and the bridge volume

$$u(a,1)+u(a,ab)=\frac{2h}{R_+},$$

$$v(a,1)+v(a,ab)=\frac{\Omega}{\pi R_+^3}. \tag{A33}$$

Excluding R_+, we have a single equation for a,

$$\tilde{\omega}(a)\equiv 4\frac{v(a,1)+v(a,ab)}{[u(a,1)+u(a,ab)]^3}=\frac{\Omega}{\pi 2h^3}, \tag{A34}$$

which is completely analogous to Eq. (A22).

It is clear that this equation always has a pair of solutions, corresponding to the two identical bridges reflected with respect to $z=0$. If one solution is $a=a_+$, then the other solution $a=a_-$ can be obtained by replacing R_+ by R_-, keeping $A=a_+R_+=a_-R_-$ the same. Since both $R_-=\rho(-h)$ and $R_+=\rho(h)$ are two roots of Eq. (A12), we have $R_-R_+=AB$, and thus, $a_-=R_+/B=1/b$, given by Eq. (A16). Obviously, the left-hand side of Eq. (A34) as a function of a has an extremum $\partial\tilde{\omega}(a)/\partial a=0$ at the point when both solutions coincide $a=a_+=a_-=1/b$. The numerical investigation shows that it is actually an absolute minimum. Since for this solution $R_-=R_+$, it belongs to the previously studied family of symmetric solutions for $a=1/b$. Thus, the radius of the inflection point $\rho=\pm\sqrt{AB}$ corresponds to the dimensionless parameter $r=\sqrt{ab}=1$, which means that the inflections are exactly at the ends of the interval $\pm h$. Condition $ab=1$ and Eq. (A16) give

$$a=a_c=\frac{1-\cos\Theta}{\sin\Theta}=\tan\frac{\Theta}{2}, \tag{A35}$$

which is the point at which a family of symmetric solutions bifurcates in two asymmetric solutions.

Now we will show that for $a>a_c$ there are no inflection points in the interval $[-h,+h]$, and that for $a<a_c$ there are exactly two inflection points. When $a>\sin\Theta$, the curvature is negative and the surface is a nodoid, which does not have inflection points. When $a=\sin\Theta$, the surface is a catenoid, also with no inflections. Finally, when $\tan\Theta/2<a<\sin\Theta$, Eq. (A16) gives $ab>1$, and the inflection point is outside the interval $[-h,h]$, because $u(a,r)$ is a monotonically increasing function of r. Analogously, if $a<\tan\Theta/2$, there are two inflection points in the profile at $r=\sqrt{ab}<1$ which are inside the interval $[-h,h]$.

6. Investigation of the second variation

In order to rigorously test the stability of the liquid bridge, we need to make sure that the solutions of Eq. (A8), corresponding to a_1 and a_2, provide the conditional minimum of the functional (A3). The equation of the second variation for this functional is

$$\delta^2 F = \int_{-h}^{h} [\delta'^2 f(z) - \delta^2 g(z)] dz, \tag{A36}$$

where

$$f(z) = \rho(1+\rho'^2)^{-3/2} = \rho(H\rho + C/\rho)^3,$$

$$g(z) = \rho^{-1}(1+\rho'^2)^{-1/2} = H + C/\rho^2, \tag{A37}$$

and $\delta(z)$ is a small arbitrary variation orthogonal to $\rho(z)$,

$$\int_{-h}^{h} \delta(z)\rho(z) dz = 0, \tag{A38}$$

such that

$$\delta'(h) = \delta'(-h) = 0. \tag{A39}$$

The orthogonality condition (A38) comes from the condition of volume constancy,

$$\pi \int_{-h}^{h} [\delta(z) + \rho(z)]^2 dz = \Omega. \tag{A40}$$

The boundary conditions (A39) follow from the condition that both $f(z)$ and $f(z)+\delta(z)$ must have the same contact angle at $z=\pm h$. In order to find out if $\delta^2 F > 0$, we need to minimize the functional (A36) with an additional condition Eq. (A38) and a normalization condition

$$\int_{-h}^{h} \delta^2(z) dz = \epsilon > 0. \tag{A41}$$

This minimization gives the second-order differential equation for δ,

$$-(\delta' f)' - g\delta + \nu\rho = \mu\delta, \tag{A42}$$

where ν and μ are Lagrangian multipliers. The multiplier ν allows one to satisfy the orthogonality condition, while multiplier μ plays the role of the eigenvalue of the correspondent selfadjoined operator $L\delta \equiv -(\delta' f)' - g\delta$ on the subset of functions orthogonal to ρ and allows one to satisfy boundary conditions (A39). If the minimal eigenvalue μ_0 is positive, $\delta^2 F = \epsilon\mu_0 > 0$ and the bridge is stable. If $\mu_0 < 0$, its eigenfunction gives $\delta^2 F = \epsilon\mu_0 < 0$, which means that the free energy decreases if we alternate the bridge profile by the corresponding eigenfunction $\delta_0(z)$. If $\mu_0 = 0$, we have a case of marginal stability, which usually separates families of stable and unstable solutions. To solve this problem numerically, one must find the solution of the homogeneous equation with $\nu=0$ and the solution of the inhomogeneous equation with $\nu=1$, which both satisfy the boundary condition $\delta'(-h)=0$. Next, one must find their linear combination, which is orthogonal to ρ. Finally, to find μ_0, one must vary μ starting from the lower bound $\mu > -g(z_0) = -1/A$, and find the value at which $\delta(h)' = 0$.

It is possible to find $\delta_0(z)$ corresponding to $\mu=0$ analytically using the identity [23]

$$2\frac{\partial H}{\partial x} = \frac{\partial \mathcal{E}(\rho)}{\partial x} = \rho^{-1} L \frac{\partial \rho}{\partial x}, \tag{A43}$$

which can be proven by direct differentiation of Eq. (A6) by an arbitrary parameter x. Selecting $x=z$, we see that $\delta(z)=\rho'(z)$ satisfies Eq. (A42) with $\nu=0$, $\mu=0$; it is always orthogonal to $\rho(z)$ for even $\rho(z)$ $[\rho(-z)=\rho(z)]$, and it satisfies the boundary conditions if $\rho''(-h)=\rho''(h)=0$, i.e., if $a=a_c$. Thus, the case $a=a_c$ corresponds to the marginal stability of the bridge which is destroyed by the antisymmetric variation of the bridge profile $\delta_a(z)=\rho'(z)$ corresponding to the infinitesimal translation of the bridge toward one of the planes.

Selecting $x=a$, we see that $\delta(z)=\partial\rho(z,a)/\partial a$ satisfies Eq. (A42) with $\nu=0$, $\mu=0$, and the boundary conditions (A39) if $\rho(z,a)$ belongs to the family of symmetric solutions. Moreover, for $a=a_0$ it also satisfies the orthogonality condition since at this point $\partial\Omega/\partial a \equiv \pi\int_{-h}^{h}\rho(z)\partial\rho(z)/\partial a dz = 0$. Thus, the case $a=a_0$ also corresponds to the marginal stability of the bridge, which is destroyed by the symmetric variation of the bridge profile $\delta_s(z)=\partial\rho(z)/\partial a$. The above considerations indicate that both a_0 and a_c play a special role in the stability of the bridge, but they do not prove that eigenvalue $\mu=0$ observed for these values of a is indeed the lowest eigenvalue μ_0.

Solving Eq. (A42) by Runge-Kutta method for all values of Θ between 0 and $\pi/2$ with a step of 1 degree, we find the eigenvalues and eigenfunctions for symmetric and antisymmetric solutions. For asymmetric solutions, as well as for other solutions having several inflection points, μ_0 is always negative. These numerical results are in complete agreement with Vogel's stability condition (ii). For a symmetric solution, $\mu_0 > 0$ if and only if $a > \max(a_c, a_0)$. If $a=a_c > a_0$, the eigenfunction $\delta_0(z)$ corresponding to $\mu_0=0$ is antisymmetric. If $a=a_0 > a_c$, the eigenfunction $\delta_0(z)$ is symmetric. This means that the bridge is stable if and only if $a > \max(a_0, a_c)$. The stability of the bridge is destroyed by the antisymmetric variation if $a_c > a_0$. If $a_c < a_0$, the bridge is destroyed by a symmetric variation. The narrow neck solution $a_1 < a_0$ is always unstable. Since for $a > a_0$ the dimensionless volume $\omega(a)$ is a monotonically increasing function of a and the average curvature H is a monotonically decreasing function of a, the fact of instability of the narrow neck bridge is in complete agreement with Vogel's stability condition $\partial\Omega/\partial H < 0$.

Both a_0 and a_c are known functions of Θ, determined by Eqs. (A29) and (A35), respectively. Thus, the type of instability that destroys the bridge depends on the contact angle Θ. Numerical studies show that the equation $a_c(\Theta)=a_0(\Theta)$ has only one root $\Theta_c \approx 31°$. For $\Theta > \Theta_c$, we have $a_c > a_0$, and the bridge breaks due to antisymmetric instability, while for $\Theta < \Theta_c$ we have $a_c < a_0$ and the bridge breaks due to symmetric instability. Substituting $a_c = \tan\Theta/2$ into Eq. (A29), we see that Θ_c must satisfy the equation

$$-2\tan(\Theta_c)\tilde{F}\left(\frac{\sqrt{\cos\Theta_c}}{\cos^2(\Theta_c/2)}, \frac{\pi-\Theta_c}{2}\right) + \frac{[7+\cos(2\Theta_c)]\cos^2(\Theta_c/2)}{2\sin^3(\Theta_c/2)\cos\Theta_c}\tilde{E}\left(\frac{\sqrt{\cos\Theta_c}}{\cos^2(\Theta_c/2)}, \frac{\pi-\Theta_c}{2}\right) - 2\cot(\Theta_c/2) = 0. \tag{A44}$$

Using Landen transformations [34–36], one can show that

$$\tilde{F}\left(\frac{\sqrt{\cos\Theta_c}}{\cos^2(\Theta_c/2)},\frac{\pi-\Theta_c}{2}\right)=K(\cos\Theta_c)\cos^2(\Theta_c/2) \tag{A45}$$

and

$$\tilde{E}\left(\frac{\sqrt{\cos\Theta_c}}{\cos^2(\Theta_c/2)},\frac{\pi-\Theta_c}{2}\right)=\frac{1}{4\cos^2(\Theta_c/2)}[2E(\cos\Theta_c) - \sin^2(\Theta_c)K(\cos\Theta_c)-2\cos(\Theta_c)], \tag{A46}$$

where $K(k)=F(k,\pi/2)$ and $E(k)=E(k,\pi/2)$ are complete elliptic integrals of the first and the second kind, respectively. Thus, Eq. (A44) is equivalent to

$$E(\cos\Theta_c)(3+\cos^2\Theta_c)-2\sin^2\Theta_c K(\cos\Theta_c)-4\cos\Theta_c=0, \tag{A47}$$

which is derived in Ref. [20] and yields $\Theta_c=31.146\,031\,127^\circ=0.54\,360\,079\,209$. The condition $\Omega/2\pi h^3>\omega(a_c)$ determines the limit of stability of the bridge only for $\Theta>\Theta_c$. For $\Theta<\Theta_c$, the condition $\Omega/2\pi h^3>\omega(a_0)$ holds.

Using Landen transformations, one can simplify the expressions for $\Lambda(a_c)$, $\sigma(a_c)$, and $\upsilon(a_c)$ for $a_c=\tan(\Theta/2)$, which are useful for determining the free energy and maximal separation between the planes for $\Theta>\Theta_c$,

$$\Lambda(a_c)=[E(\cos\Theta)-\cos\Theta]/\sin\Theta, \tag{A48}$$

$$\sigma(a_c)\equiv\sigma(a_c,1)=2E(\cos\Theta)/\sin^2\Theta-K(\cos\Theta) - 2\cos\Theta/\sin^2\Theta, \tag{A49}$$

and

$$\upsilon(a_c)\equiv\upsilon(a_c,1)=\frac{1}{12\sin^3\Theta}[-33\cos\Theta+\cos 3\Theta + 2(15+\cos 2\Theta)E(\cos\Theta)-16K(\cos\Theta)\sin^2\Theta]. \tag{A50}$$

Thus, for $\Theta>\Theta_c$, the maximal separation between the planes for which the bridge is mechanically stable, is given by

$$\eta_{\rm ms}=\Lambda(a_c)/[2\pi\upsilon(a_c)]^{1/3}, \tag{A51}$$

which is expressed in compete elliptic integrals and trigonometric functions. For $\Theta<\Theta_c$,

$$\eta_{\rm ms}=\Lambda(a_0)/[2\pi\upsilon(a_0,1)]^{1/3}, \tag{A52}$$

where a_0 is the root of the transcendental equation (A29), and where $\Lambda(a_0)=u(a_0,1)$ and $\upsilon(a_0,1)$ are expressed in incomplete elliptic integrals given by Eqs. (A26) and (A27).

For $\Theta=90^\circ$, the bridge is a cylinder, so $\rho(z)$ is constant and the solutions of Eq. (A42) are sines and cosines. After elementary calculations, one can find that the antisymmetric variation $\delta=\sin(\pi z/2h)=\sin(z/\rho)$ is the eigenfunction corresponding to the minimal eigenvalue $\mu_0=0$ at $\eta=\pi^{1/3}/2$, corresponding to the Carter conjecture [27], while the symmetric variation $\delta=\cos(\pi z/h)=\cos(2z/\rho)$ gives $\mu_1=3\pi/h>0$. At $\eta=(\pi/2)^{1/3}$ coinciding with the limit of the maximal separation of the planes for the family of symmetric solutions $\lim_{\Theta\to\pi/2}\eta(a_0)$, the symmetric solution gives $\mu_1=0$, while the antisymmetric solution has already negative $\mu_0=-3\pi/(4h)$.

In general, for $\Theta>\Theta_c$ and for small enough dimensionless plane separation $\eta\leqslant\eta_{\rm ms}$, we have $\mu_s>\mu_a\geqslant 0$, where μ_s and μ_a are the lowest eigenvalues of the symmetric and antisymmetric solutions, respectively. At $\Theta<\Theta_c$, the eigenvalues switch the order and we have $\mu_a>\mu_s\geqslant 0$. Exactly at $\Theta=\Theta_c$, both eigenvalues become zero at the same $\eta=\eta_{\rm ms}$.

7. Free energy

The above analysis predicts that for large contact angles $\Theta>\Theta_c$, the bridge must break into one droplet or into two unequal droplets by translation toward one of the planes, while for $\Theta<\Theta_c$, the bridge must break symmetrically right in the middle, producing two equal droplets on the opposite planes.

Once the liquid bridge is broken, it will form one or two droplets attached to one of the planes with contact angle Θ. This droplet will acquire a shape of a spherical segment of radius R_0, with the center at $(x=0,\ y=0,\ z=\pm[h+R_0\cos\Theta])$ forming a circular intersection with the plane of the radius $\rho_0=R_0\sin\Theta$. In the case of one resulting droplet,

$$R_0=\left[\frac{6\Omega}{2\pi(2-3\cos\Theta+\cos^3\Theta)}\right]^{1/3}. \tag{A53}$$

If the breaking of the bridge generates two identical droplets, the above equation must be multiplied by $2^{-1/3}$. The minimal separation of the planes in the case of one droplet is

$$2h_{\min,1}=R_0(1-\cos\Theta). \tag{A54}$$

In the case of two droplets, it is

$$2h_{\min,2}=2^{2/3}R_0(1-\cos\Theta). \tag{A55}$$

Interestingly, these distances coincide with the plane separations in the limiting case $a\to 0$ of the unstable asymmetric and symmetric solutions, respectively, which—as it follows from the numerical studies of Eq. (A28)—have larger free energies than the wide neck symmetric solution for the same volume. Moreover, this wide neck solution has $a_2>a_c$, and hence is stable. This suggests that as soon as a droplet intersecting one of the planes touches the opposite plane, it forms a symmetrical bridge. The same is true for two droplets intersecting the opposite planes if they touch each other. Indeed, since the area of the spherical surface of the droplet is

$$S_{0,1}=\pi R_0^2 2(1-\cos\Theta), \tag{A56}$$

the surface free energy of the single droplet is

$$\mathcal{F}_{0,1}=\pi\gamma R_0^2[2(1-\cos\Theta)-\sin^2\Theta\cos\Theta]. \tag{A57}$$

The surface free energy of the two equal droplets is $\mathcal{F}_{0,2}=\mathcal{F}_{0,1}2^{1/3}$. Both of these quantities are larger than $\mathcal{F}[a_2(\omega_k)]$, where $a_2(\omega_k)$ is the largest solution of Eq. (A22) for $\omega_k=\Omega/2\pi h_{\min,k}$. Moreover, numerical analysis shows

that $h_{\min,2} < h_{\mathrm{ms}}$, thus the mechanically stable bridge will form as soon as the droplets on the opposite planes touch each other, or the opposite plane.

For any Θ, we can find the maximal distance $2h_s$, for which the bridge is thermodynamically stable, solving the equation $\mathcal{F}(h_s) = \mathcal{F}_{0,1}$. This equation has only one solution for $a > \max(a_0, a_c)$. The complete phase diagram of the bridges with $\Theta < \pi/2$ is presented in Fig. 9.

Finally, we will find the free energy release $\Delta\mathcal{F}$ during rupture of the bridge as the difference between the free energies of the closed and opened states. Since the pathway of rupture changes from breaking into two equal droplets for $\Theta < \Theta_c$, to breaking into one droplet or two unequal droplets for $\Theta > \Theta_c$, the free energy release will change from $\Delta\mathcal{F} = \mathcal{F}(a_c) - \mathcal{F}_{0,1}$ for $\Theta \gg \Theta_c$ to $\Delta\mathcal{F} = \mathcal{F}(a_0) - \mathcal{F}_{0,2}$ for $\Theta \leqslant \Theta_c$, where $\mathcal{F}(a_0)$ and $\mathcal{F}(a_c)$ are defined by Eq. (A28), in which $\sigma(a,1)$ is given by Eqs. (A25) and (A49), respectively (see Fig. 10). Since for $\Theta > \Theta_c$, the bridge may break into two unequal droplets, whose total free energy is in between $\mathcal{F}_{0,2}$ and $\mathcal{F}_{0,1}$, we can expect that $\Delta\mathcal{F}$ is a continuous function of Θ. The exact pathway of the bridge breaking in the overdamp limit can be found by the conjugate gradient method, in which for each unstable bridge profile $\rho(z)$, a small variation $\delta(z)$ of fixed norm, orthogonal to $\rho(z)$ and minimizing $\delta\mathcal{F}$, is found.

[1] Rayleigh, Lord, Philos. Mag. **34**, 145 (1879).
[2] M. P. Mahajan, M. Tsige, S. Zhang, J. I. Alexander, P. L. Taylor, and C. Rosenblatt, Phys. Rev. Lett. **84**, 338 (2000).
[3] M. Heil and J. P. White, J. Fluid Mech. **462**, 79 (2002).
[4] D. Langbein, F. Falk, and R. Grossbach, Advances in Space Research **16**(7), 23 (1995).
[5] N. S. Bhatt, M. R. Dodge, J. I. Alexander, L. A. Slobozhanin, P. L. Taylor, and C. Rosenblatt, Phys. Rev. E **65**, 026306 (2002).
[6] L. A. Slobozhanin, J. I. D. Alexander, and V. D. Patel, Phys. Fluids **14**, 209 (2002).
[7] R. D. Kamm and R. C. Schroter, Respir. Physiol. **75**, 141 (1989).
[8] D. P. Gaver III, R. W. Samsel, and J. Solway, J. Appl. Physiol. **69**, 74 (1990).
[9] D. R. Otis, F. Petak, Z. Hantos, J. J. Fredberg, and R. D. Kamm, J. Appl. Physiol. **80**, 2077 (1996).
[10] D. P. Gaver III, D. Halpern, O. E. Jensen, and J. B. Grotberg, J. Fluid Mech. **319**, 25 (1996).
[11] A. M. Alencar, S. Arold, S. V. Buldyrev, A. Majumdar, D. Stamenović, H. E. Stanley, and B. Suki, Nature (London) **417**, 809 (2002).
[12] Z. Hantos, J. Tolnai, A. M. Alencar, A. Majumdar, and B. Suki, J. Appl. Physiol. **97**, 592 (2004).
[13] R. T. H. Laënnec, *De l'Auscultation Médiate ou Traité du Diagnostic de Maladies des Poumons et du Coeur, Fondé Principalement sur ce Nouveau Moyen d'Exploration* (Brosson et Chaudé, Paris, 1819).
[14] R. L. H. Murphy, Jr., S. K. Holford, and W. C. Knowler, N. Engl. J. Med. **296**, 968 (1977).
[15] D. Halpern and J. B. Grotberg, J. Fluid Mech. **244**, 615 (1992).
[16] H. Pasterkamp, S. S. Kraman, and G. R. Wodicka, Am. J. Respir. Crit. Care Med. **156**, 974 (1997).
[17] A. M. Alencar, Z. Hantos, F. Peták, J. Tolnai, T. Asztolos, S. Zapperi, J. S. Andrade, Jr., S. V. Buldyrev, H. E. Stanley, and B. Suki, Phys. Rev. E **60**, 4659 (1999).
[18] A. M. Alencar, S. V. Buldyrev, A. Majumdar, H. E. Stanley, and B. Suki, Phys. Rev. Lett. **87**, 088101 (2001).
[19] J. J. Fredberg and S. K. Holford, J. Acoust. Soc. Am. **3**, 1036 (1983).
[20] D. Langbein, *Capillary Surfaces: Shape-Stability-Dynamics, in Particular Under Weightlessness*, Springer Tracts in Modern Physics (Springer-Verlag, Berlin, 2002).
[21] R. Finn, *Equilibrium Capillary Surfaces* (Springer-Verlag, New York, 1985).
[22] T. I. Vogel, SIAM J. Appl. Math. **47**, 516 (1987).
[23] T. I. Vogel, SIAM J. Appl. Math. **49**, 1009 (1989).
[24] R. Finn and T. I. Vogel, Z. Anal. Ihre Anwend. **11**, 3 (1992).
[25] L. Zhou, Pac. J. Math. **178**, 185 (1997).
[26] M. Athanassenas, J. Reine Angew. Math. **377**, 97 (1987).
[27] W. C. Carter, Acta Metall. **36**, 2283 (1988).
[28] N. Metropolis and S. Ulam, J. Am. Stat. Assoc. **44**, 335 (1949).
[29] K. Binder and D. W. Heermann, *Monte Carlo Simulation in Statistical Physics, An introduction* (Springer, Berlin, 1997).
[30] K. Kawasaki, *Phase Transition and Critical Phenomena* (Academic Press, New York, 1972).
[31] D. P. Landau and K. Binder, *A Guide to Monte Carlo Simulation in Statistical Physics* (Cambridge University Press, New York, 2000).
[32] K. Huang, *Statistical Mechanics* (Wiley, New York, 2004).
[33] V. I. Smirnov, *A Course of Higher Mathematics, Vol. 4: Variational Calculus* (Pergamon Press, Oxford, 1964).
[34] *Handbook of Mathematical Functions*, edited by M. Abramowitz and I. A. Stegun (Dover, New York, 1970).
[35] N. I. Akhiezer, *Elements of the Theory of Elliptic Functions* (American Mathematical Society, Providence, 1990).
[36] I. S. Gradshtein and I. M. Ryzhik, *Table of Integrals, Series and Products*, 5th ed. (Academic Press, San Diego, 1994).